Published in final edited form as:
Anal Chem. 2012 October 16; 84(20): 8837–8845. doi:10.1021/ac3022423.

Microsphere Degradation in Outer Hydrogel Membranes Creates Macroscopic Porosity to Counter Biofouling-Induced Sensor Degradation

S. Vaddiraju[#1,2], **Y. Wang**[#3], **L. Qiang**[1], **D. J. Burgess**[3,*], and **F. Papadimitrakopoulos**[1,4,*]

[1] Polymer Program, Institute of Materials Science, University of Connecticut, Storrs, CT 06269-3136.

[2] Biorasis Inc. Technology Incubation Program, University of Connecticut, Storrs, CT 06269-4213

[3] Department of Pharmaceutical Sciences, University of Connecticut, Storrs, CT 06269-3092

[4] Department of Chemistry, University of Connecticut, Storrs, CT 06269-3060

[#] These authors contributed equally to this work.

Abstract

Biofouling and tissue inflammation present major challenges toward the realization of long-term implantable glucose sensors. Following sensor implantation, proteins and cells adsorb on sensor surfaces to not only inhibit glucose flux but also signal a cascade of inflammatory events that eventually lead to permeability-reducing fibrotic encapsulation. The use of drug-eluting hydrogels as outer sensor coatings has shown considerable promise to mitigate these problems via the localized delivery of tissue response modifiers to suppress inflammation and fibrosis, along with reducing protein and cell absorption. Biodegradable poly (lactic-co-glycolic) acid (PLGA) microspheres encapsulated within a poly (vinyl alcohol) (PVA) hydrogel matrix, presents a model coating where the localized delivery of the potent anti-inflammatory drug dexamethasone has been shown to suppress inflammation over a period of 1-3 months. Here it is shown that the degradation of the PLGA microspheres provides an auxiliary venue to offset the negative effects of protein adsorption. This was realized by: *1)* the creation of fresh porosity within the PVA hydrogel following microsphere degradation (which is sustained until the complete microsphere degradation); and *2)* rigidification of the PVA hydrogel to prevent its complete collapse onto the newly created void space. Incubation of the coated sensors in PBS buffer led to a monotonic increase in glucose permeability (50%), with a corresponding enhancement in sensor sensitivity over a one-month period. Incubation in serum resulted in biofouling and consequent clogging of the hydrogel microporosity. This however, was partially offset by the generated macroscopic porosity following microsphere degradation. As a result of this, a two-fold recovery in sensor sensitivity for devices with microsphere/hydrogel composite coatings was observed as opposed to similar devices with blank hydrogel coatings. These findings suggest that the use of macroscopic porosity can reduce sensitivity drifts resulting from biofouling and this can be achieved synergistically with current efforts to mitigate negative tissue responses through localized and sustained drug delivery.

[*] Corresponding authors: d.burgess@uconn.edu, papadim@mail.ims.uconn.edu.

INTRODUCTION

Implantable amperometric sensors for continuous monitoring of glucose hold promise for the care and management of diabetes.[1] A major obstacle to the development of these sensors arises from their poor *in vivo* stability.[2] This occurs as a consequence of the foreign body response (FBR) following device implantation, which involves a series of events that starts with the adsorption of proteins and cells and eventually leads to the formation of a fibrotic capsule around the implant.[3, 4] Such action causes a significant reduction in analyte permeability towards the sensing element, which is initially manifested as a gradual loss in sensor sensitivity and eventually leads to a total loss of device functionality.[5, 6] To this effect, small molecules and protein fragments generated as part of the FBR, play an important role in not only adsorbing onto various interfaces (*i.e.* electrodes and outer coatings)[7] but also in aggregating within semipermeable membranes of the sensor that eventually leads to pore clogging.[8]

Attempts to improve *in vivo* sensor stability include the elimination of surface biofouling (*i.e.* the random and dynamic adsorption of proteins on the implant).[9-11] For this, advanced coatings based on biofouling-resistant, hydrogel membranes have shown promise in slowing down protein adsorption.[12, 13] Unfortunately, the 'static' nature of these hydrogels eventually succumb to biofouling, since the implant is constantly challenged with fresh proteins, protein fragments and ions.[12-14] 'Active' strategies to mitigate biofouling include the use of nanoporous hydrogels that change their permeability in response to various stimuli (*i.e.* temperature,[15, 16,17] magnetic[18] and electric fields[19]). These strategies employ reversible expansion and contraction to assist in dislodging of the surface-adsorbed proteins.[15, 16, 18, 19] While their successes are somewhat limited,[10, 11] additional challenges may also arise during their incorporation within the 3D architectures of implanted sensors.

Localized delivery of tissue response modifiers (TRMs) has shown considerable promise in suppressing inflammation and fibrosis. Sensor coatings for sustained delivery of various TRMs such as the anti-inflammatory drug dexamethasone,[20-25] growth factors (e.g. VEGF and PDGF[26, 27]), vasodilator agents (like NO[28-32]) and combinations thereof have been reported. The efficacy of these approaches stems from the sustained TRM(s) delivery throughout the lifetime of the implant.[22] To this end, our group has shown that drug-delivery composite coatings based on poly-(lactic-co-glycolic acid) (PLGA) microspheres and PVA hydrogels form an ideal combination in lieu of sustained TRM release via the use of different populations of microspheres.[21] In addition, the composite membranes possess mechanical integrity that matches tissue stiffness and cushions the hard implant against the soft tissue.[33] Furthermore, the PVA hydrogel has the ability to store supplemental amount of oxygen (necessary for improved sensor linearity),[34] while at the same time displaying ample permeability to small analytes.[34, 35] While inflammation and fibrosis has been successfully countered for up to 3 months via the local delivery of the potent anti-inflammatory drug dexamethasone,[21] biofouling remains an issue.[5, 36, 37] Proteins, protein fragments and ions adsorbed on various sensor elements can possibly degrade sensor performance due to: (a) permeability changes of hydrogels and possibly other semipermeable membranes;[5-7] (b) surface contamination of active electrodes;[7, 8] (c) enzyme deactivation;[7] as well as (d) offset in the balance of glucose to O_2 ratio.[38] In order to minimize biofouling-induced sensor degradation, one has to devise strategies that counter all these undesirable effects.

With this in mind, our group has recently developed a stacked-layer sensor architecture that progressively limits the diffusion of larger molecular weight species towards the working electrode. As shown in Figure 1, the working electrode is covered with a self-sealing, electropolymerized polyphenol (PPh) thin film to limit the diffusion of species larger than H_2O_2 (*i.e.* uric acid, ascorbic acid, acetaminophen and various low molecular weight protein

fragments).[35, 39] This innermost layer, aside from imparting high sensor selectivity (greater than 97%), also prevents the deposition of contaminants onto the working electrode[40, 41] in the unlikely event that they pass through the various outer layers of the sensor. Following the glucose oxidase (GO_x) containing second layer, the 1-2 μm Selectophore polyurethane (PU) third layer provides the second diffusion limiting barrier to the sensor.[35] The segmented nature of this PU with 35% of crystallization-prone hydrophobic content and 65% of medium hydrophilicity poly(tetramethylene oxide) micro-domains significantly slows down glucose diffusion (as opposed to oxygen) to afford superior sensor linearity.[35] Moreover, this PU layer substantially impedes the inner diffusion of hydrophilic protein fragments with sizes greater than glucose. Accordingly, the effects of biofouling are mostly concentrated at the outer PVA layer (both on its surface and inside crevices) and to a lesser extent on the PU/PVA interface. This permits us to study biofouling-induced reduction in hydrogel permeability and develop strategies against it.

In this contribution, we report a simple, yet versatile venue to minimize hydrogel biofouling via incorporation of biodegradable microspheres. Following incubation in phosphate buffered saline (PBS) and in porcine serum, changes in permeability and sensitivity from sensors coated with outer PLGA microsphere/PVA hydrogel composite coatings are directly related to the generation of macroscopic porosity resulting from microsphere degradation. Such macroscopic porosity is shown to offset the biofouling-induced permeability reduction via hydrogel pore clogging. The origin of macroscopic porosity stems from the incomplete collapse of the PVA hydrogel following microsphere degradation. This is further augmented through PVA rigidification by the adsorbed ions and proteins present in serum.

EXPERIMENTAL

2.1. Materials

Glucose oxidase enzyme (GO_x) (157,500 units/g activity, Aspergillus Niger[42]), glutaraldehyde (25% w/v solution in water), phenol, bovine serum albumin (BSA), glutaraldehyde (50% w/v), *D*-glucose and dexamethasone were purchased from Sigma. PVA (99% hydrolyzed, MW 133 kDa) was obtained from Polysciences Inc. (Warrington, PA). Polyurethane was purchased from Fluka (catalog number 81367, Selectophore). Platinum and silver wires were purchased from World Precision Instruments. Poly (lactic-co-glycolic acid) (PLGA) resomer RG503H 50:50 (MW 25kDa, carboxylic acid end capped) were gifts from Boehringer-Ingelheim and Purdue Pharma. Methylene chloride was obtained from Fisher Scientific.

2.2. Experimental methods

Dexamethasone-loaded microspheres were prepared by an oil-in-water emulsion solvent extraction/evaporation technique as described previously.[33] In brief, 2 g PLGA were dissolved in 8 ml methylene chloride followed by dispersing 200 mg of dexamethasone in the same solution. This organic phase was emulsified in 40 ml of a 1% (w/w) PVA (average MW: 30 to 70 KDa) solution and homogenized at 10,000 rpm for 1.5 min using a Power Gen 700D homogenizer (Fisher Scientific, Pittsburgh, PA). The resultant emulsion was poured into 500 ml of a 0.1% (w/w) PVA solution and stirred under vacuum to achieve rapid evaporation of methylene chloride. The hardened microspheres were washed three times with de-ionized water and collected by filtration (0.45 μm). The prepared microspheres were kept under vacuum overnight and later stored at 4 °C until further use. The average size of the microspheres is about 7 ± 3 μm.[43]

Coil-type glucose sensors were fabricated as described previously.[34, 35, 44] In brief, the working electrode was coated with a thin (*ca.* 10 nm) layer of polyphenol, electropolymerized from a 100 mM aqueous phenol solution at 0.8 V *vs.* Ag/AgCl

reference.[39] Subsequently, a layer of glucose oxidase (GO_X)/bovine serum albumin (BSA) was dip-coated and immobilized *via* glutaraldehyde crosslinking, followed by 2-hr soaking in phosphate buffered saline (PBS) pH 7.4 to remove uncrosslinked protein[45] and to ensure no long term leaching of GO_X. The GO_X-coated sensor were then immediately dip-coated with a polyurethane (PU) layer from a 3% (w/w) PU solution in 98% tetrahydrofuran (THF)/ 2% dimethylformamide (DMF) (w/w).[39] Subsequently, the entire device was coated with a PVA hydrogel with or without dexamethasone-loaded PLGA microsphere aqueous suspension (75 mg PLGA microspheres per ml of PVA solution) and subjected to three freeze-thaw cycles to induce physical PVA crosslinking.[33, 34]

Amperometric response experiments were performed in stirred solutions of either PBS (pH 7.4) or porcine serum maintained at 37 °C and under an applied potential of 0.7 V *vs.* an Ag/ AgCl reference electrode using a CH Instruments (Model CHI1010A) electrochemical analyzer. After an initial background stabilization period of 500 seconds, the concentration of glucose was sequentially raised to 30 mM (*via* steps of 2 mM) and the amperometric response was continuously recorded. *In vitro* sensitivity is determined as the slope of the linear regression between sensor response and glucose concentration for the entire concentration range tested.

Long-term sensor response experiments were performed by incubating the sensors in either PBS buffer or in porcine serum containing 5.6 mM glucose, maintained at 37 °C. The solutions were renewed periodically to prevent possible bacterial growth (at least twice a week). The sensitivities of the sensors were obtained by measuring the sensor responses to sequential glucose increments from 5.6 mM to 13.1 mM in three increments of 2.5 mM, yielding four data points within the hyperglycemic range. The sensors were also checked periodically (by sequential increments of glucose from 2 mM to 25 mM) to ensure that they retained their full physiological range linearity throughout the course of this study.

In vitro glucose permeability data were obtained using a Franz cell apparatus maintained at 37 °C.[46] PVA membranes (with and without dexamethasone-loaded PLGA microspheres) were cast in a Teflon mold and physically crosslinked via three freeze-thaw cycles. These membranes were carefully peeled from the mold, immersed in PBS (pH 7.4) for 3 hr to attain equilibrium swelling and sandwiched between the donor and receiver chambers of the Franz cell. For permeability experiments in PBS, the receiver chamber contained blank PBS solution while the donor chamber contained 1M glucose in PBS solution. In the case of permeability experiments in porcine serum, the receiver and donor chambers were filled with porcine serum containing 5.6 mM and 1M glucose, respectively. Subsequently, glucose diffused from the donor to the receiver chamber through the PVA membrane. The glucose concentrations in the donor and receiver chambers were deduced using a home-made glucose sensor. The diffusion coefficient of glucose through the membrane was deduced using equations 1 and 2.[47]

$$\ln\left(\frac{C_D - C_R}{C_{D0} - C_{R0}}\right) = -\beta D_e t \quad (1)$$

$$\beta = \frac{A}{l}\left(\frac{1}{V_D} + \frac{1}{V_R}\right) \quad (2)$$

wherein β is the cell constant, D_e is the effective diffusion coefficient; C_{Do} and C_{Ro} are the initial glucose concentrations in the donor and receiver chambers, respectively; C_D and C_R are the glucose concentrations at time t in the donor and receiver cells, respectively; A is the

area of diffusion; l is the membrane thickness; and V_D and V_R are the volumes of donor and receiver cells, respectively.

Sensor Morphology was determined using scanning electron microscopy (SEM) on a JOEL JSM-6335F, operating at 10 kV accelerating voltage with a 15 mm working distance between the final condenser lens and the specimen. Samples before and after long-term stability testing, were dried and sputter-coated with Pd to eliminate charging during imaging.

In vitro dexamethasone release profiles from the PLGA microsphere/PVA hydrogel composite coatings were obtained as described elsewhere.[48]

RESULTS

Figure 1 illustrates schematically the cross-section of our basic electrochemical glucose sensor.[35] The low porosity of the inner polyphenol (PPh) layer not only imparts greater than 97% sensor selectivity against common interferences (*i.e.* acetaminophen, ascorbic acid, uric acid) but also impedes electrode fouling by blocking the passage of small molecular weight contaminants (*i.e.* small molecular weight amines that are known to electropolymerize on Pt electrode and reduce sensitivity[49]) This selectivity is achieved at operating potential as high as 0.7 V *vs.* Ag/AgCl reference and is retained for more than 4 weeks.[35, 39] Following the GO_x enzyme layer, the device is coated with a conformal 1-2 μm film of another semipermeable membrane composed of Selectophore polyurethane (PU). The segmented nature of this PU (with 35% of hydrophobic and crystallization-prone methylene bis-p-cyclohexyl isocyanate/butane diol segments and 65% of the medium hydrophilic poly (tetramethylene oxide) micro-domains) plays a dual role: *(i)* the large hydrophobic content promotes greater oxygen diffusion against the larger hydrophilic glucose. This offsets the large glucose-to-O_2 ratio within the *s.c.* tissue (typically 30 to 300 in normal *vs.* hyperglycemic conditions) and renders the sensor linear over the entire physiological glucose concentration range (2 to 22 mM);[35, 50] and *(ii)* selectively impede the inner diffusion of protein segments significantly larger than the size of glucose. This prevents large proteins and protein fragments to diffuse in towards the GO_x enzyme layer and deactivate it as well as biofoul the innermost PPh film.

The entire device was encased within a thick (*ca.* 100 μm when in dry state) poly(vinyl alcohol) (PVA) hydrogel that contain dexamethasone-loaded poly(lactic-*co*-glycolic acid) (PLGA) microspheres. The PVA hydrogel provides a continuous hydrophilic pathway for glucose to diffuse inwards as well as for the GO_x-catalyzed byproducts to diffuse outwards.[34] On the other hand, the hydrophobic PLGA microspheres locally release dexamethasone through their gradual degradation,[33] which is schematically shown in Figure 1 with three vertical sections corresponding to an idealized case of 0, 7, and 30 days incubation. In Figure 1, the hydrogel is depicted as non-collapsing following microsphere degradation, which is expected to increase its glucose permeability. However, a partial collapse is more realistic.

Figure 2a illustrates the typical dexamethasone release profile from a one month study of the PLGA microsphere/PVA hydrogel composite coating. This release profile consists of three phases: an initial burst release (days 1 to 3) resulting from release of surface associated drug, followed by a lag phase (days 4-12) in which microsphere degradation sets in, that leads to a zero-order release phase (day 13 onwards) where the PLGA entrapped dexamethasone slowly diffuses out. The burst release phase typically accounts for approximately 40% of dexamethasone release, with the remaining drug released between days 10 and 35.

Figure 2b illustrates the sensor response *vs.* glucose concentration for devices coated with only polyurethane (PU) as well as those encased within a PVA hydrogel matrix with and without PLGA microspheres. All three devices were tested after 3-hr incubation in PBS buffer maintained at 37 °C to ensure complete swelling of the PVA coating.[33] As can be seen in Figure 2b, the PU coating by itself is sufficient to impart a linear amperometric response for glucose concentrations well beyond the physiological (2 to 22 mM) range. The addition of the PVA hydrogel on top of the PU membrane did not hinder sensor linearity but slightly lowered sensor sensitivity by *ca.* 20%. The inclusion of PLGA microspheres within the PVA hydrogel (indicated as PU + PVA/PLGA device) resulted in a further 20% decrease in the amperometric response. These results suggest that the PVA hydrogel in its pristine form (*i.e.* not exposed to protein), presents a barrier to the diffusion of glucose towards the GO_x enzyme, which is directly translated to sensor sensitivity.

Figure 3 superimposes the variations in glucose permeability through PVA films (with and without PLGA microspheres) along with the corresponding sensor sensitivity as a function of incubation time in PBS buffer containing 5.6 mM glucose, over a period of 30 days. In the case of the PVA hydrogel coatings alone (Figure 3a), both the glucose flux (top) and sensor sensitivity (bottom) remained fairly constant over the 30-day test period. In the case of the composite PLGA microsphere/PVA hydrogel outer membranes (Figure 3b), both glucose flux (top) and sensor sensitivity (bottom) exhibited a steady increase with time. The trends in Figure 3b appear to resemble the drug release profile shown in Figure 2a, particularly after 5-7 days when the PLGA degradation begins to set in. This indicates that following microsphere degradation, the formation of macroscopic porosity leads to a corresponding increase in sensor sensitivity. Overall by day 30, the glucose flux and the sensor sensitivity increased from their initial values by 50% and 70%, respectively.

Figure 3c illustrates the sensor response *vs.* glucose concentration for devices coated with either blank PVA hydrogels or microsphere-loaded PVA hydrogel composites, before (day one) and after a 30-day incubation period in PBS. In all four cases, excellent device linearity is retained over the entire physiological glucose range. In terms of sensor sensitivity, the 30-day incubation period in PBS caused a minute increase (less than 10%) for devices coated with blank PVA hydrogels, which can be contrasted with the significant increase (more than 60%) for sensors coated with the composite microsphere/hydrogels.

Figure 4 depicts SEM micrographs of sensors coated with PVA hydrogels (with and without the PLGA microspheres) on days one and 30 following incubation in PBS. On day one, the surfaces of the PVA coated devices were relatively smooth with no visible pores (Figure 4a). Barring the fact that the surface of the day 30 device (Figure 4b) became smoother than that of the day one device (probably due to swelling-induced hydrogel redistribution around the coils of the working electrode (clearly shown in Figure 4a)), no other significant change occurred. In the case of the microsphere/hydrogel composite-coated devices (Figures 4c) the presence of the microspheres (both as individuals and aggregates) gave a bristly appearance to the sensor surfaces on day one. The mean particle size of the microspheres, as deduced from Figure 4c and other SEM micrographs was slightly larger (*ca.* 19 ± 7 μm) than that of the starting microspheres (*ca.* 7 ± 3 μm[43]). This indicates that the most of the microspheres were aggregated and surrounded by PVA hydrogel. Upon incubation in PBS for 30 days (Figure 4d), the bristly appearance was replaced with a large amount of dimples (shown by the black-headed arrows) and crevices (indicated by the white-headed arrows). The dimples probably arise from partially PVA-coated microspheres that have been dislodged. The crevices are macroscopic voids that are believed to originate from degradation of microspheres that were completely surrounded by the PVA hydrogel. The presence of crevices indicates that the PVA hydrogel does not collapse completely after microsphere

degradation. This provides a visual confirmation of generated macroscopic porosity that was inferred from the increased glucose flux shown in Figure 3b.

Having established that in simple buffer solution, microsphere degradation within PVA hydrogels enhances glucose permeability, the long-term performance of the composite coatings was investigated following incubation in serum. Exposure to serum was expected to result in surface biofouling by proteins, ions and small molecules. Figure 5 illustrates the variation in glucose permeability and sensor sensitivity (right and left ordinate, respectively) as a function of incubation time in serum containing 5.6 mM of glucose, over a period of 30 days. It is important to note that these amperometric experiments and glucose diffusion studies were carried out without exposing the sensor to other media. This avoids any possible rinse-induced protein desorption from the sensor surfaces.[51]

Exposing the PVA hydrogel coatings to serum resulted in an initial rapid decrease in glucose permeability of approximately 60% (top curve in Figure 5a) until day 9, after which the glucose permeability remained fairly constant. The corresponding sensor sensitivity (bottom curve in Figure 5a) showed a similar rapid decrease of approximately 56% until day 9, and continued to decrease at a lower rate until day 30 resulting in an approximately 70% decrease overall. The similarity in the magnitude of the initial decrease for both the permeability and sensitivity up to day 9 indicates an association with PVA biofouling.

In the case of the composite PLGA microsphere/PVA hydrogel membranes, the glucose permeability (top curve in Figure 5b) showed a markedly different trend as compared to sensors coated with blank PVA hydrogels. Two cycles of permeability increase and decrease were evident between days 0 to 9 and between days 9 to 30. The steepness of the first cycle was larger than that of the second. The two ascending segments are probably associated with the generation of macroscopic porosity during the burst release phase (when surface associated drug is released) and during the zero-order release phase (when microsphere degradation/elimination occurs). The two descending segments are likely to result from biofouling induced permeability reduction during the initial lag phase and at the end of the zero-order phase, respectively (Figure 2a). The sensor sensitivity trend (middle curve in Figure 5b) is markedly different than that of the permeability response (top curve). Although, the PVA/PLGA composite coated sensor sensitivity response appears similar to that of those coated with blank PVA, the following disparities are worth noting:

- **i.** The overall drop in the sensitivity of the PVA/PLGA composite coated sensors (35%) is significantly less than that for the sensors coated with blank PVA hydrogel (70%).
- **ii.** At day two the sensitivity of the PVA/PLGA composite coated sensors is equal to if not larger than their starting sensitivity. This trend is completely opposite to that of the sensors coated with blank PVA. This suggests that the observed sharp increase in permeability of the PVA/PLGA composite (top curve in Figure 5b) during the microsphere burst release phase has definite contribution in preventing sensitivity reduction due to biofouling.

Figure 5c illustrates the sensor response *vs.* glucose concentration for devices coated with either blank PVA hydrogel or PLGA microsphere/PVA hydrogel composites before and after the 30-day incubation period in serum. In all cases, excellent device linearity is retained over the entire physiological glucose range. Moreover, the 71 and 33% decrease in sensor sensitivity for the blank PVA- and PLGA microspheres/PVA hydrogel composite-coated sensors (Figure 5c) closely matches the corresponding 70 and 35% sensitivity drops observed for incubation in 5.6 mM glucose concentration (Figures 5a and 5b, respectively).

Figure 6 shows SEM micrographs of sensors coated with PVA hydrogel (with and without the PLGA microspheres) following a 30-day incubation period in serum. The following observations can be made upon comparing these images to the SEM micrographs obtained from exposure to PBS (Figure 4):

- **a.** for the blank PVA coatings, the serum appears to impede PVA redistribution over the sensor as the sensor coils are still evident at 30 days (Figure 6a); and
- **b.** for the PLGA/PVA composite coated devices (Figure 6b) a more pronounced dimple and crevice pattern is evident.

These two findings indicate that the serum exposed PVA coatings become rigidified (as a result of biofouling, similar to previous studies[52]) thus impeding PVA redistribution and preventing collapse of both dimples and crevices.

DISCUSSION

The amperometric results shown in Figure 2b and Ref. 35 indicate that the PU layer is solely responsible for limiting entry of glucose (and molecules larger than glucose) to the inner sensor membranes. The addition of PVA (with or without PLGA microspheres) forms an additional barrier to the overall glucose permeability. As a result of this, the response of the sensor is directly linked to the permeability of both the PU and PVA layers. Thus the sensor sensitivity could be affected either by biofouling or to a lesser extent by any potential swelling of the permselective PU membrane. The latter can be readily established by observing the sensitivity increase of the blank PVA-coated sensor upon incubation in PBS for 30 days (Figure 3a and 3c). The minute (less than 10%) change in sensor sensitivity of blank PVA-coated devices between days one and 30 (Figure 3c) signifies that PU swelling is almost negligible and can be safely ignored. Thus, device sensitivity can be directly linked to changes in PVA permeability resulting from microsphere erosion (Figure 2), as well as biofouling-induced surface and pore clogging of PVA and to a lesser extent protein adsorption at the PU/PVA interface. Using this model, the permeability and sensitivity changes in Figures 3 and 5 can be explained as follows:

The one-to-one correlation of permeability and sensitivity changes in PBS (Figure 3b) clearly demonstrates that in the absence of biofouling, the macroscopic porosity generated following microsphere erosion is responsible for the enhanced sensor response. While the constant increase follows the general trend of the microsphere degradation profile, as established by the dexamethasone release (Figure 2a), the inability to clearly observe the burst release and lag phases suggest that PVA is flexible enough to collapse around the degrading microspheres (as evident by the reduced contrast of dimples and crevices in Figure 4d). The latter phenomenon is also supported by the observed hydrogel redistribution around the electrode coils, following the 30-day incubation period in PBS (Figure 4a to 4b).

Incubation in serum resulted in immediate biofouling on the surface and inner pores of PVA layer. Aside from rapidly reducing glucose permeability (Figure 5a), protein adsorption also stiffens the inherent hydrogel structure, as evident from the enhanced contrast of the dimples and crevices along with the lack of PVA redistribution observed in the SEM images (Figure 6). While biofouling will gradually clog the pores, the stiffening of the hydrogel will be almost immediate. This explains the rapid initial increase in glucose permeability for the PVA/PLGA composite coatings (Figure 5b) with biofouling catching up during the lag phase of dexamethasone release (Figure 2a). Similarly, the second observed increase in glucose permeability (between days 15 and 20) coincides with the onset of the zero-order release phase of the microspheres (Figure 2a & 5b).

The aforementioned results provide an initial indication that in the presence of a stiffened hydrogel, rapid increases in macroscopic porosity can increase the overall sensor sensitivity and thus can offset the negative effect of biofouling on the sensor sensitivity. To test the validity of this model, the observed changes in sensitivity of the PVA/PLGA composite sensor (middle curve in Figure 5b) can be reconstructed by multiplying the blank PVA sensor (bottom curve in Figure 5a) with the glucose permeability of the composite layer (top curve in Figure 5b). For this, the blank-PVA sensitivity response was factored to account for the lower volume fraction of PVA in the composite (*i.e.* 40%). The bottom curve of Figure 5b shows the reconstructed trend, which closely matches the experimentally observed sensitivity trend depicted by the middle curve. This provides additional evidence that the development of macroscopic porosity can indeed offset biofouling-induced changes.

Finally, it is important to differentiate the contribution of biofouling on the PVA layer compared to the PU/PVA interface. The sensitivity response of the blank PVA-coated devices in Figure 5a shows the presence of two distinct drops; *i.e.* a rapid one between days 1 and 9 and a slower one after 15 days. From the corresponding permeability results, the lack of a second drop indicates that the first one is associated with PVA-induced protein adsorption. Consequently, the second drop must be related to the PU/PVA interface, since this interface is not present in the diffusion studies (where films of blank PVA hydrogel were utilized). The delayed biofouling response at the PU/PVA interface can be understood in terms of the slow displacement dynamics of the PVA hydrogel at the PU interface. The fact that the second drop is only 14% of the overall 70% sensitivity decrease for the blank-PVA device indicates that the adhesion of PVA hydrogel onto the PU layer is sufficiently strong to inhibit complete biofouling of the PU layer. This is an important finding since gains due to generation of macroscopic porosity through microsphere degradation will not be ultimately compromised by biofouling at PU/PVA interface.

CONCLUSIONS

It has been demonstrated that PLGA microsphere degradation within a PVA hydrogel matrix generates fresh macroscopic porosity that can lead to an increase in glucose permeability, which in turn is translated to enhancement in sensor sensitivity. SEM studies indicate that the generation of such macroscopic porosity stems from an incomplete collapse of the PVA hydrogel. In the presence of serum, hydrogel collapse is further reduced by PVA rigidification due to protein adsorption. The creation of macroscopic porosity following microsphere degradation was shown to offset the negative effect of protein-induced pore clogging with the net result of a significant reduction in the loss of sensor sensitivity in the presence of serum. This renders the concept of macroscopic porosity generation as a relatively simple method to offset biofouling-induced sensitivity drifts following sensor implantation. This can be achieved through microsphere degradation that also provides sustained release of tissue response modifying drugs to suppress acute and chronic inflammation and prevent fibrotic sensor encapsulation. Future studies are aimed to better understand the interplay between hydrogel rigidification and macroscopic porosity generation (in both biofouling and non-biofouling media) as well as evaluating the efficacy of the concept *in vivo* and in well-controlled *ex vivo* environments (such as a media containing proteins, protein fragments and cells).

Acknowledgments

Financial support for this study was obtained from US Army Medical Research Grants (W81XWH-09-1-0711 and W81XWH-07-10688), NIH grants (1-R21-HL090458-01, R43EB011886 and 9R01EB014586) and NSF/SBIR grant (1046902).

REFERENCES

1. Kerner W. Expt. Clin. Endocrinol Diabetes. 2001; 109:S341–S346.
2. Wilson, GS.; Zhang, Y. In In vivo glucose sensing. Cunningham, DD.; Stenken, JA., editors. John Wiley & Sons; Hoboken: 2009.
3. Anderson JM. Annu Rev Mater Res. 2001; 31:81–110.
4. Anderson JM, Rodriguez A, Chang DT. Semin Immunol. 2008; 20:86–100. [PubMed: 18162407]
5. Wisniewski N, Moussy F, Reichert WM. Fresenius J. Anal. Chem. 2000; 366:611–621. [PubMed: 11225773]
6. Gerritsen M, Jansen JA, Kros A, Vriezema DM, Sommerdijk NAJM, Nolte RJM, Lutterman JA, Van Hövell SWFM, Van der Gaag A. J. Biomed. Mat. Res. 2001; 54:69–75.
7. Linke B, Kiwit M, Thomas K, Krahwinkel M, Kerner W. Clinical Chem. 1999; 45:283–285.
8. Kerner W, Kiwit M, Linke B, Keck FS, Zier H, Pfeiffer EF. Biosens. Bioelectron. 1993; 8:473–482. [PubMed: 8311940]
9. Koh A, Nichols SP, Schoenfisch MH. J Diabetes Sci Technol. 2011; 5:1052–1059. [PubMed: 22027297]
10. Vaddiraju S, Burgess DJ, Tomazos I, Jain FC, Papadimitrakopoulos F. J Diabetes Sci Technol. 2010; 4:1540–1562. [PubMed: 21129353]
11. Vaddiraju S, Tomazos I, Burgess DJ, Jain FC, Papadimitrakopoulos F. Biosens. Bioelectron. 2010; 25:1553–1565. [PubMed: 20042326]
12. Yang W, Xue H, Carr LR, Wang J, Jiang S. Biosens. Bioelectron. 2011; 26:2454–2459. [PubMed: 21111598]
13. Yang Y, Zhang SF, Kingston MA, Jones G, Wright G, Spencer SA. Biosens. Bioelectron. 2000; 15:221–226. [PubMed: 11219733]
14. Valdes T, Ciridon W, Ratner B, Bryers J. Biointerphases. 2011; 6:43–53. [PubMed: 21721839]
15. Gant RM, Abraham AA, Hou Y, Cummins BM, Grunlan MA, Coté GL. Acta Biomaterialia. 2009; 6:2903–2910. [PubMed: 20123136]
16. Gant RM, Hou Y, Grunlan MA, Coté GL. J. Biomed. Mat. Res. 2009; 90A:695–701.
17. Ding X-B, Sun Z-H, Zhang W-C, Peng Y-X, Wan G-X, Jiang Y-Y. J. Applied Poly. Sci. 2000; 77:2915–2920.
18. Ainslie KM, Sharma G, Dyer MA, Grimes CA, Pishko MV. Nano Letters. 2005; 5:1852–1856. [PubMed: 16159237]
19. Yeh PY, Le Y, Kizhakkedathu JN, Chiao M. Biomed. Microdevices. 2008; 10:701–708. [PubMed: 18427993]
20. Ju YM, Yu B, West L, Moussy Y, Moussy F. J. Biomed. Mat. Res. 2010; 93:200–210.
21. Bhardwaj U, Sura R, Papadimitrakopoulos F, Burgess DJ. Intl. J. Pharm. 2010; 384:78–86.
22. Bhardwaj U, Sura R, Papadimitrakopoulos F, Burgess DJ. J. Diabetes Sci. Technol. 2007; 1:8–17. [PubMed: 19888374]
23. Hickey T, Kreutzer D, Burgess DJ, Moussy F. J. Biomed. Mat. Res. 2002; 61:180–187.
24. Hickey T, Kreutzer D, Burgess DJ, Moussy F. Biomaterials. 2002; 23:1649–1656. [PubMed: 11922468]
25. Patil SD, Papadimitrakopoulos F, Burgess DJ. Diabetes Tech. Therapeutics. 2004; 6:887–897.
26. Patil SD, Papadimitrakopoulos F, Burgess DJ. J. Controlled Release. 2007; 117:68–79.
27. Norton LW, Koschwanez HE, Wisniewski NA, Klitzman B, Reichert WM. J. Biomed. Mat. Res. 2007; 81:858–869.
28. Hetrick EM, Prichard HL, Klitzman B, Schoenfisch MH. Biomaterials. 2007; 28:4571–4580. [PubMed: 17681598]
29. Hetrick EM, Schoenfisch MH. Chem. Soc. Rev. 2006; 35:780–789. [PubMed: 16936926]
30. Shin JH, Schoenfisch MH. Analyst. 2006; 131:609–615. [PubMed: 16795923]
31. Frost MC, Batchelor MM, Lee Y, Zhang H, Kang Y, Oh B, Wilson GS, Gifford R, Rudich SM, Meyerhoff ME. Microchemical Journal. 2003; 74:277–288.
32. Frost MC, Meyerhoff ME. Methods in Enzymology. 2004; 381:704–715. [PubMed: 15063707]

33. Galeska I, Kim TK, Patil SD, Bhardwaj U, Chatttopadhyay D, Papadimitrakopoulos F, Burgess DJ. AAPS Journal. 2005; 07:E231–E240. [PubMed: 16146344]
34. Vaddiraju S, Singh H, Burgess DJ, Jain FC, Papadimitrakopoulos F. J. Diabetes Sci. Technol. 2009; 3:863–874. [PubMed: 20144336]
35. Vaddiraju S, Legassey A, Wang Y, Qiang L, Burgess D, Jain F, Papadimitrakopoulos F. J Diabetes Sci. Technol. 2011; 5:1044–1051. [PubMed: 22027296]
36. Wisniewski N, Klitzman B, Miller B, Reichert WM. J. Biomed. Mat. Res. 2001; 57:513–521.
37. Wisniewski N, Reichert M. Colloids and Surfaces B: Biointerfaces. 2000; 18:197–219.
38. Wilson GS, Gifford R. Biosens. Bioelectron. 2005; 20:2388–2403. [PubMed: 15854814]
39. Chen X, Matsumoto N, Hu Y, Wilson GS. Anal. Chem. 2002; 74:368–372. [PubMed: 11811410]
40. Geise RJ, Adams JM, Barone NJ, Yacynych AM. Biosens. Bioelectron. 1991; 6:151–160.
41. Sasso SV, Pierce RJ, Walla R, Yacynych AM. Anal. Chem. 1990; 62:1111–1117.
42. Wilson R, Turner APF. Biosens. Bioelectron. 1992; 7:165–185.
43. Rawat A, Burgess DJ. Intl. J. Pharm. 2010; 394:99–105.
44. Vaddiraju S, Burgess DJ, Jain FC, Papadimitrakopoulos F. Biosens. Bioelectron. 2008; 24:1557–1562. [PubMed: 18823767]
45. House JL, Anderson EM, Ward WK. J. Diabetes Sci. Technol. 2007; 1:18–22. [PubMed: 19888375]
46. Bourke SL, Al-Khalili m. Briggs T, Michniak BB, Kohn J, Poole-Warren LA. AAPS PharmSci. 2003; 5:101–111.
47. Praveen SS, Hanumantha R, Belovich JM, Davis BL. Diabetes Technol. Therapeutics. 2003; 5:393–399.
48. Zolnik BS, Raton JL, Burgess DJ. Dissolution Tech. 2005; 12:11–14.
49. Qiang L, Vaddiraju S, Rusling JF, Papadimitrakopoulos F. Biosens. Bioelectron. 2010; 26:682–688. [PubMed: 20655730]
50. Qiang L, Vaddiraju S, Patel D, Papadimitrakopoulos F. Biosens. Bioelectron. 2011; 26:3755–3760.
51. Koschwanez HE, Reichert WM. Biomaterials. 2007; 28:3687–3703. [PubMed: 17524479]
52. Fussell G, Thomas J, Scanlon J, Lowman A, Marcolongo M. Journal of Biomaterials Science, Polymer Edition. 2005; 16:489–503. [PubMed: 15887655]

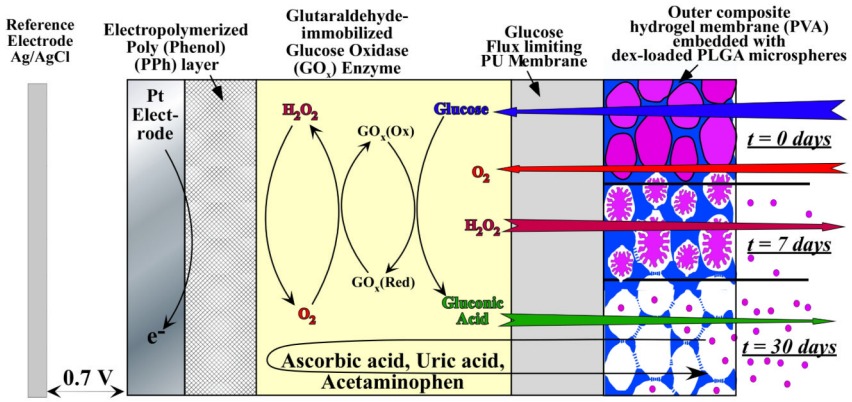

Figure 1.

Schematic cross-section of the sensor under investigation in this study (layer thicknesses are not to scale). The outer composite hydrogel coating shows embedded PLGA microspheres at different stages of degradation. At day 7 & 30, following microsphere degradation the PVA hydrogel is shown to be non-collapsing, which leads to the generation of macroscopic porosity at the microsphere/hydrogel interface.

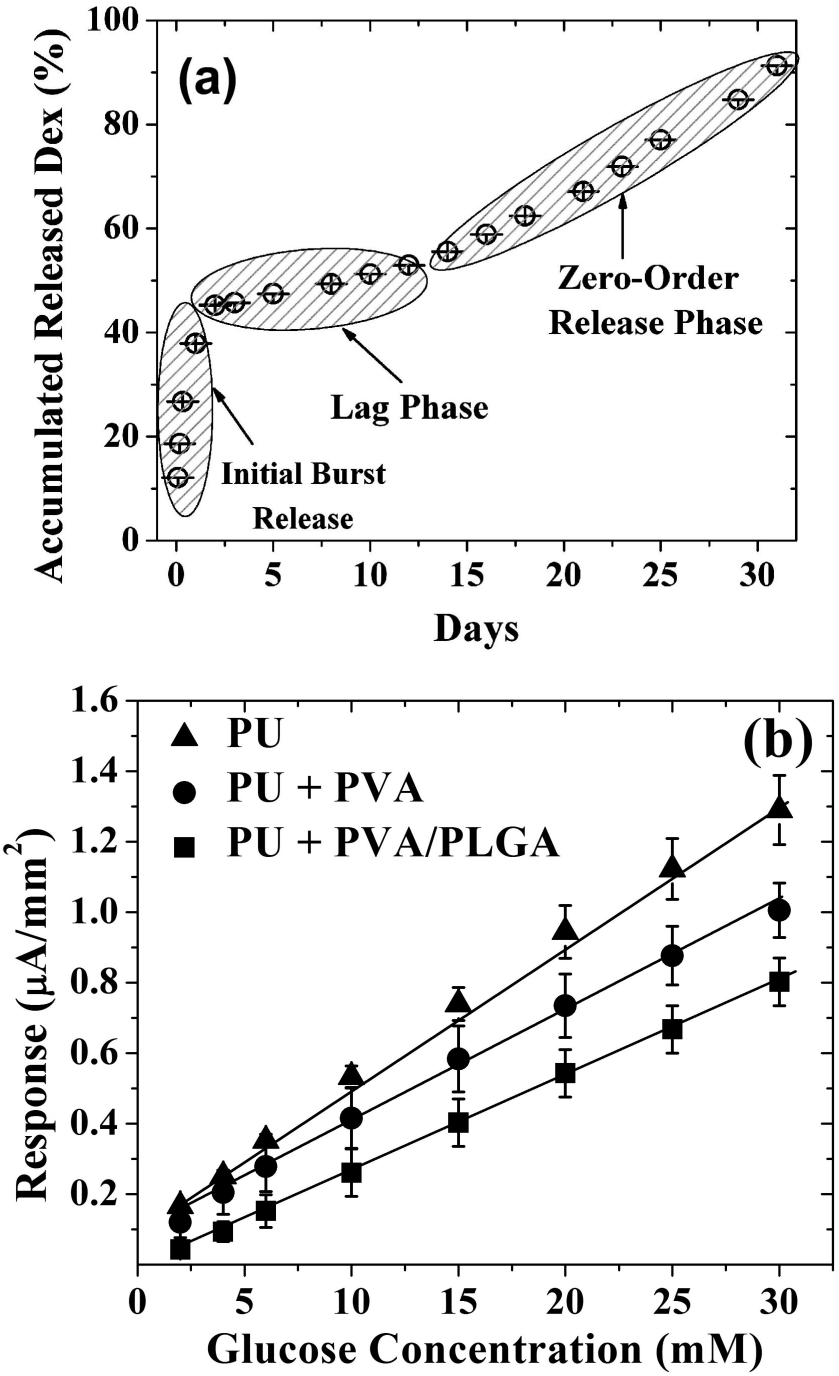

Figure 2.

(a) Release profile of dexamethasone from the outer composite hydrogel membrane (PVA), embedded with dexamethasone-loaded microspheres, as schematically shown in the outer most layer of Figure 1. **(b)** Saturation amperometric current *vs.* glucose concentration for devices coated with PU, PU+blank PVA and PU+PLGA/PVA composite coatings.

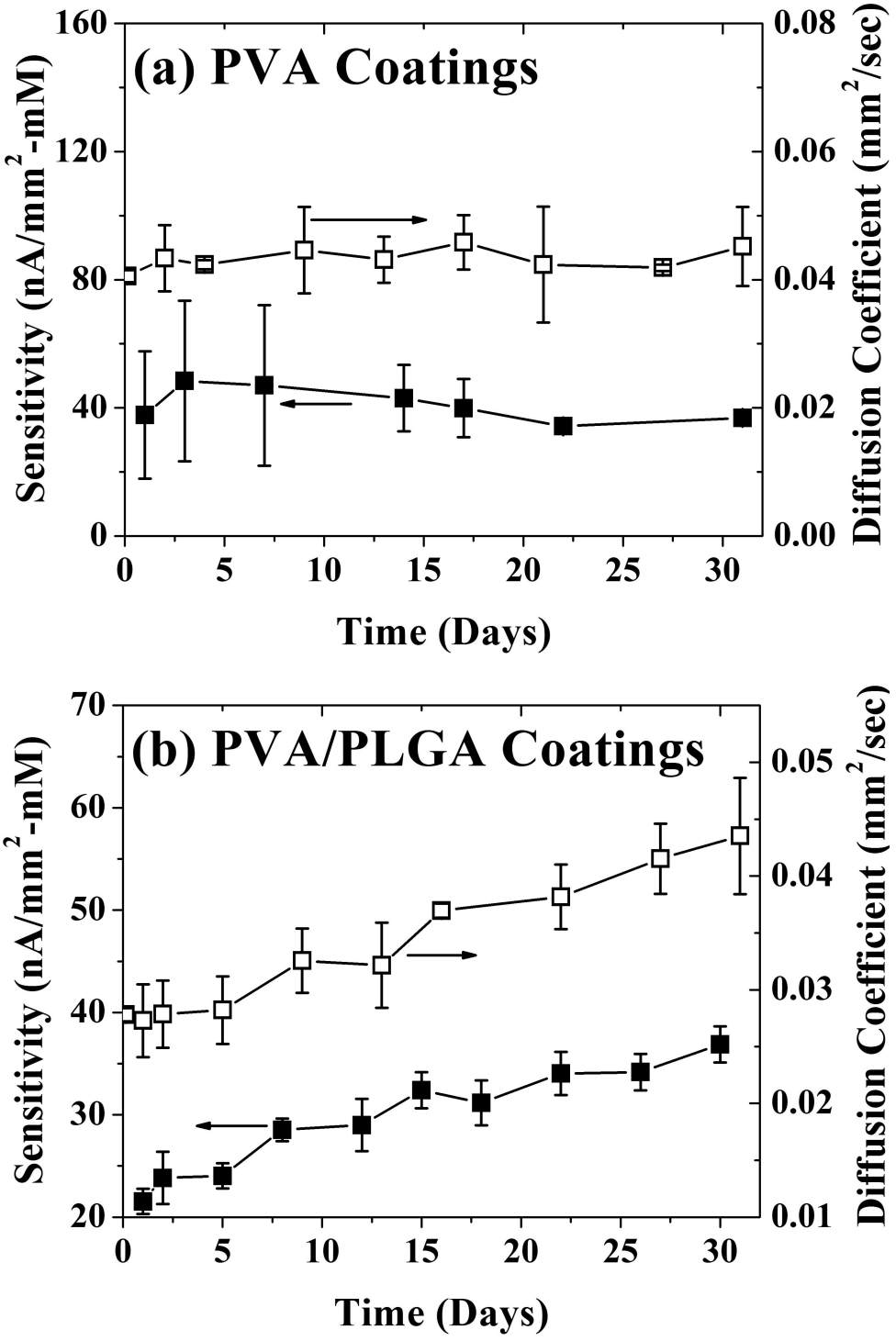

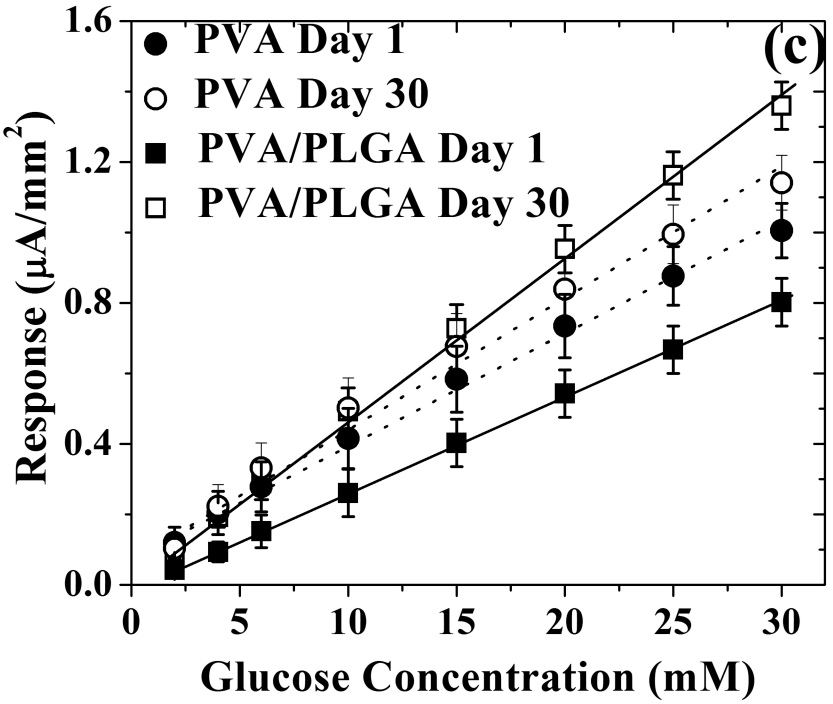

Figure 3.

Sensor sensitivity (left ordinate) and glucose permeability (right ordinate) as a function of incubation time in PBS buffer containing 5.6 mM of glucose for **(a)** blank PVA hydrogel and **(b)** composite coating of PLGA microspheres in PVA hydrogel. **(c)** Saturation amperometric sensor response *vs.* glucose concentration for sensors coated with blank PVA hydrogel (dotted lines, circle symbols) and composite coating of PLGA microsphere/PVA hydrogel (solid lines, square symbols) before (day 1) and after 30 day incubation in PBS buffer containing 5.6 mM of glucose.

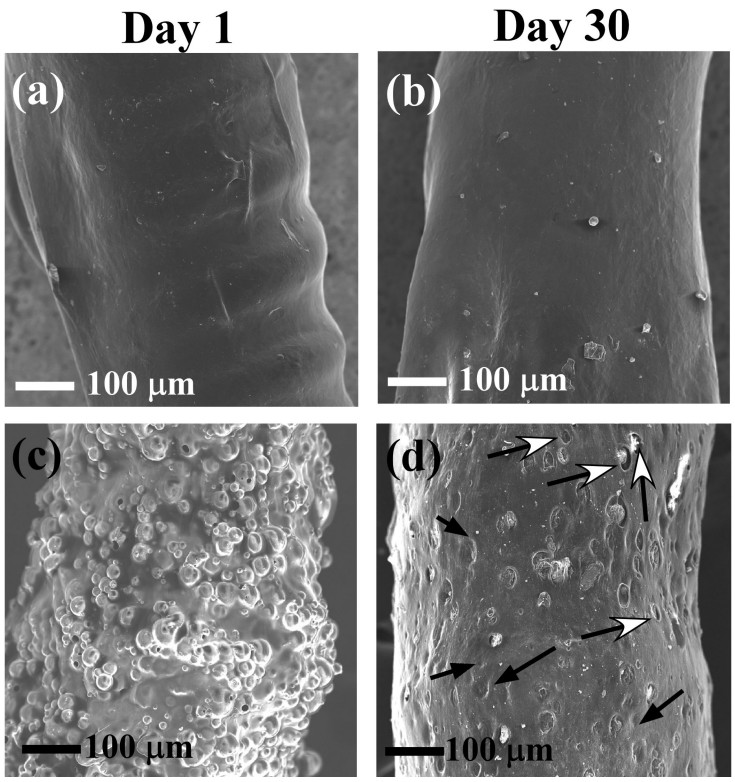

Figure 4.
SEM images of the PVA hydrogel-coated (a, b) and PLGA microspheres/PVA hydrogel composite-coated (c, d) devices at day 1 (a, c) and day 30 (b, d) following incubation in PBS buffer solution (pH 7.4) containing 5.6 mM of glucose.

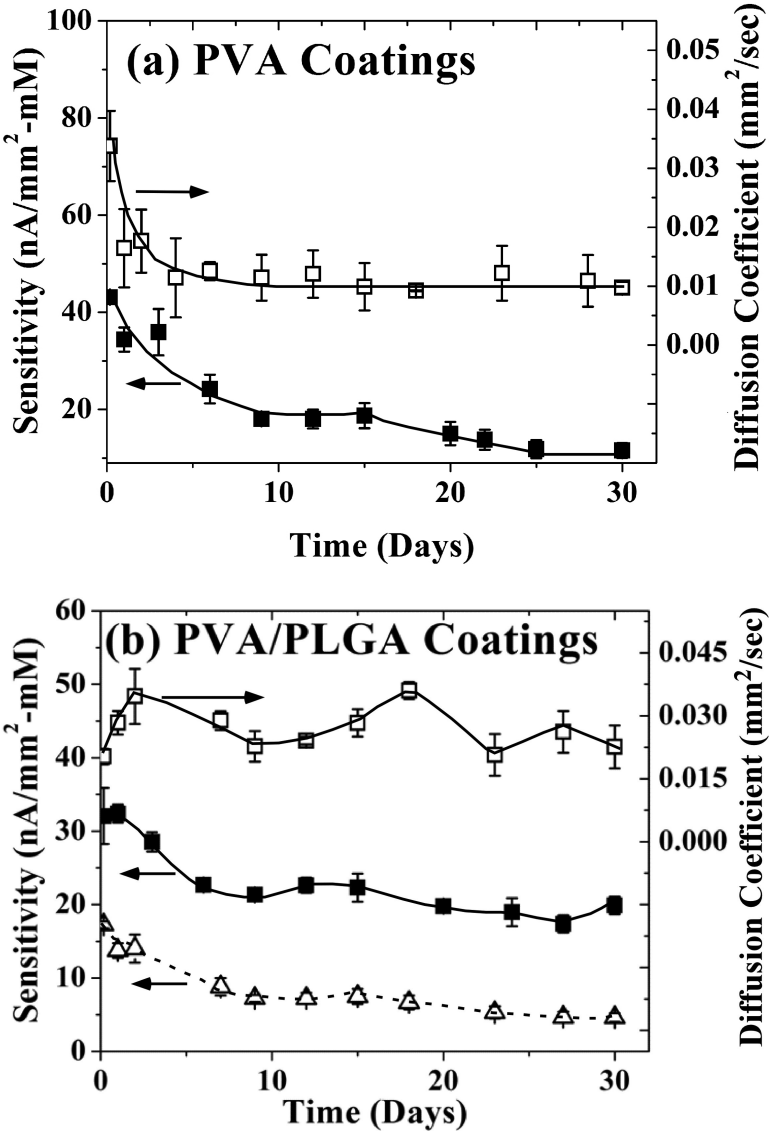

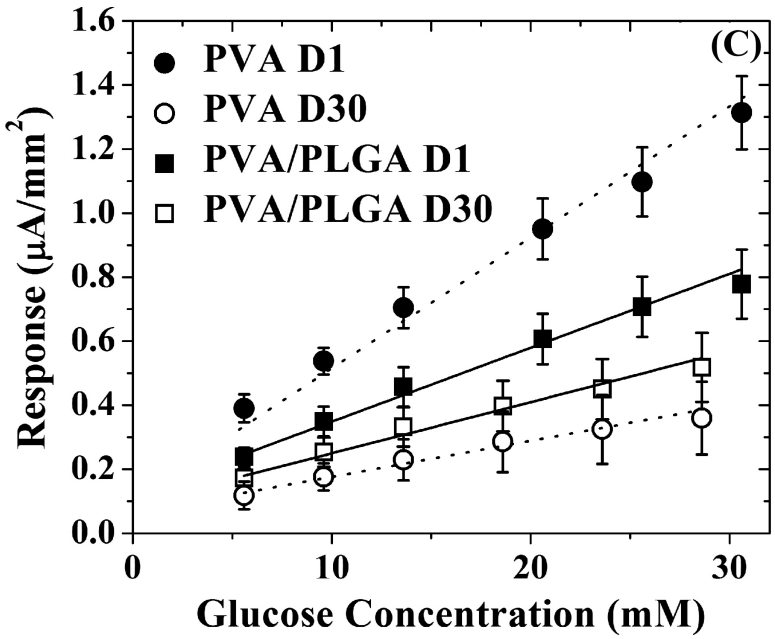

Figure 5.

Sensor sensitivity (left ordinate) and glucose permeability (right ordinate) as a function of incubation time in porcine serum containing 5.6 mM of glucose for **(a)** blank PVA hydrogel and (b) composite coating of PLGA microspheres in PVA hydrogel. The bottom dotted curve in **(b)** depicts the re-constructed trend in sensitivity utilizing the volume ratio factored sensitivity response of the blank PVA-coated device (bottom curve of (a)) multiplied by the permeability changes in the PVA/PLGA composite (top curve of (b)). **(c)** Saturation amperometric sensor response *vs.* glucose concentration for sensors coated with blank PVA hydrogel (dotted lines, circle symbols) and composite coating of PLGA microsphere/PVA hydrogel (solid lines, square symbols) before (day 1) and after 30 day incubation in porcine serum containing 5.6 mM of glucose.

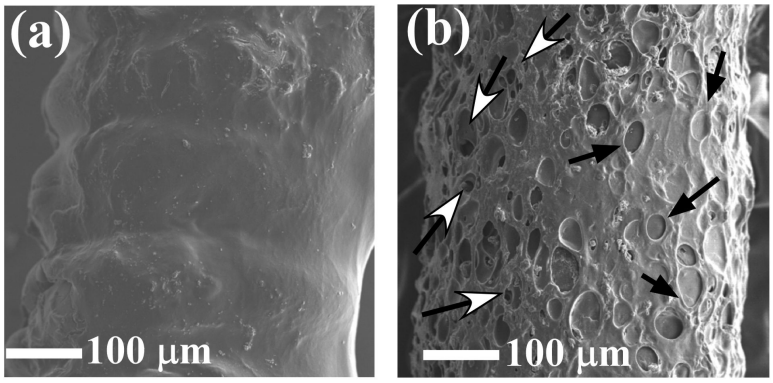

Figure 6.
SEM images of the PVA hydrogel-coated (a) and PLGA microspheres/PVA hydrogel composite-coated (b) devices at day 30, following incubation in porcine serum containing 5.6 mM of glucose.